small NANO MICRO

Detection of Nitric Oxide from Living Cells Using Polymeric Zinc Organic Framework-Derived Zinc Oxide Composite with Conducting Polymer

*Min-Yeong Kim, Malenahalli Halappa Naveen, Nanjanagudu Ganesh Gurudatt, and Yoon-Bo Shim**

Sensitive and selective detection of nitric oxide (NO) in the human body is crucial since it has the vital roles in the physiological and pathological processes. This study reports a new type of electrochemical NO biosensor based on zinc-dithiooxamide framework derived porous ZnO nanoparticles and polyterthiophene-rGO composite. By taking advantage of the synergetic effect between ZnO and poly(TTBA-rGO) (TTBA = 3′-(p-benzoic acid)-2,2′:5′,2″-terthiophene, rGO = reduced graphene oxide) nanocomposite layer, the poly(TTBA-rGO)/ZnO sensor probe displays excellent electrocatalytic activity and explores to detect NO released from normal and cancer cell lines. The ZnO is immobilized on a composite layer of poly(TTBA-rGO). The highly porous ZnO offers a high electrolyte accessible surface area and high ion–electron transport rates that efficiently catalyze the NO reduction reaction. Amperometry with the modified electrode displays highly sensitive response and wide dynamic range of 0.019–76 × 10^{-6} M with the detection limit of 7.7 ± 0.43 × 10^{-9} M. The sensor probe is demonstrated to detect NO released from living cells by drug stimulation. The proposed sensor provides a powerful platform for the low detection limit that is feasible for real-time analysis of NO in a biological system.

1. Introduction

Nitric oxide (NO) is a long-elusive endothelium regulation relaxing factor in diverse biological processes,[1] such as signal transductions in the central nervous system, an integral part of the immune system, inflammatory response, modulations of ion channels, and cardiovascular homeostasis.[2,3] Earlier, NO was only known to be a toxic pollutant; however, it received immense research interest after the discovery of NO functions in the biological system.[4] Monitoring of NO concentrations in a biological system is crucial due to its several functions in the human body. The quantification of trace NO is difficult because of its short half-life and spontaneous chemical reactivity.[5] Therefore, various analytical approaches for monitoring NO level in very low concentration have been proposed employing mainly spectroscopic and electrochemical methods.[6] Spectroscopic methods, however, have some limitations that are indirect measurements of by-products of NO species and direct measurement of adducts formed between NO and metal complexes, fluorescent dyes, or spin traps.[7] Although high sensitivity and selectivity were observed in some spectroscopic methods, the most of these techniques are difficult to miniaturize and demand sophisticated instrument. On the other hand, electrochemical methods offer direct analysis in high sensitivity, selectivity, and reproducible analytical performance; they are inexpensive and simple operation.[8] However, the electrochemical

M.-Y. Kim, Dr. M. H. Naveen, N. G. Gurudatt, Prof. Y.-B. Shim
Department of Chemistry
Pusan National University
Busan 46241, Republic of Korea
E-mail: ybshim@pusan.ac.kr

DOI: 10.1002/smll.201700502

system demands an adequate electrode material or the modification of electrode surface, which is crucial to achieving selectivity and sensitivity. Thus, various electrocatalytic materials have been proposed such as metal/metal oxide nanoparticles (NPs), carbon materials, conducting polymers (CPs), and proteins/enzymes. Of these, metal oxides are considered as one of the promising candidates of nonenzymatic electrocatalytic materials for the sensing devices.

To date, various types of metal and metal oxides, such as Fe, Zn, Cu, Mn, Co, and Ni, have been reported for electrochemical applications.[9] Among these, zinc oxide (ZnO) has received special attention due to its potential applications in photovoltaics and semiconducting, and they had been used as catalysts for some chemical and biomolecule detection.[10–13] Thus, various methods have been proposed for the preparation of ZnO NPs using surfactant assisted, templating methods, sol–gel, and various chemical deposition methods,[14] which are commonly composed of amorphous or semi-crystalline. Recently, many researchers have attempted using metal-organic frameworks (MOFs) or metal complex framework as a precursor to obtain porous metal oxide and/or porous carbon by changing the pyrolysis condition.[15,16] MOF-derived materials having high surface area and porosity are useful to improve the performance in various applications. Thus, we tried to prepare ZnO through the preparation of ZnDTO (DTO = dithiooxamide) framework. It is, however, not stable on the bare electrode substrate for analytical purpose, due to the brittle and not adhesive property of ZnO. To stabilize ZnO NPs for an electrode surface, it is possible to use the CP layer that can improve the selectivity and the stability of ZnO without loss of conductivity for sensing applications.

π-conjugated CPs are another class of electrode materials for numerous applications, such as electrochromic device, battery, solar cell, and sensor fields.[17] Especially, electrochemically polymerized CPs have great advantages in biosensor applications.[18] Of various CPs, polypyrrole, polyaniline, polythiophene, and polyterthiophene have been considered potential candidates due to their promising applications in the research fields.[19] Among them, polyterthiophene is highly stable and its derivatives have special features for modification of electrode surface in biosensor and many applications.[8,18,20] However, CPs themselves are somewhat low conductivity compared to metal. Thus, one of the ways to improve their conductivity is the incorporation of metal NPs, carbon nanotube, or graphene to the CP layer. Graphene has been one of the promising electrode materials due to its excellent conductivity and electrochemical properties,[21] so different types of graphene composites have been prepared and used in various electrochemical applications. In particular, graphene composite electrodes with CPs have displayed outstanding performance for the detection of glucose, dopamine, ascorbic acid (AA), hydrogen peroxide, and many biologically important molecules.[22] The main advantage of the graphene in the electrochemical sensor system is a large enhancement in the current response that is directly related to the sensitivity of the electrodes due to its high surface area and excellent conductivity. There are reports to show that incorporation of metal oxides (TiO_2, ZnO, MnO, etc.) on graphene exhibited excellent electrocatalytic performance for biosensor and distinct applications.[23,24] Thus, ZnO NPs attached on a graphene and CP composite layer with excellent individual properties will give enhanced performances for the biosensor devices.

In the present work, we studied, for the first time, porous ZnO particles prepared from ZnDTO framework as a new precursor, and the electrochemical NO sensor was developed using poly(TTBA-rGO)/ZnO nanocomposite. The complex formation between Zn and DTO with N and S ligating atoms gives the homogeneous spherical structure of ZnDTO framework. Thus, it was used as a precursor to prepare template free porous spherical ZnO NPs through heat treatment. Compared to other preparation methods of ZnO NPs, the ZnDTO-derived material exhibits distinct merits such as uniform size, high porosity, and well dispersed round shape NPs that can enhance the performance of the ZnO. The formation of nanocomposite was confirmed by field-emission scanning electron microscopy (FESEM), energy dispersive X-ray spectroscopy (EDX), X-ray powder diffraction (XRD), and X-ray photoelectron spectroscopy (XPS). The electrochemical activity of the electrode was studied using the cyclic voltammetry (CV), electrochemical impedance spectroscopy (EIS), and chronoamperometry techniques. The proposed poly(TTBA-rGO)/ZnO electrode was studied for the enhanced catalytic performance toward the reduction of NO and confirmed the validity of sensor through the detection of NO released from living cells.

2. Results and Discussion

2.1. Preparation and Characterization of Sensor Probe

The preparation scheme of the sensor probe is presented in **Figure 1**. Here, we for the first time tried to prepare ZnO NPs using a zinc organic framework. The zinc framework precursor was prepared by the complex formation reaction based on our previous method.[25a] The structure of ZnDTO framework was confirmed by different techniques, such as fourier transform-infrared spectroscopy (FT-IR), thermogravimetric analysis (TGA), XRD, and EDX data. In this case, FT-IR revealed the complexation between Zn and DTO. XRD spectra of ZnDTO matched with the CuDTO MOF structure.[25b] In addition, a big difference in the thermal degradation temperature between DTO and ZnDTO also confirmed the formation of polymeric complex framework. Further, EDX also confirmed the elemental composition of the ZnDTO. As shown in Figure 1, (step I) porous ZnO NPs were prepared from ZnDTO framework precursor by heat treatment at 700 °C. By modifying the preparation conditions, two different sizes of ZnDTO particles were prepared for smaller and bigger ZnO NPs. To attain porous ZnO NPs, the synthesized ZnDTO was subjected to pyrolysis in a tube furnace for 3 h under open air condition. Morphology and particle size of the precursor ZnDTO framework and the ZnO NPs were confirmed by FESEM and transmission electron microscopy (TEM) measurements. The FESEM images displayed the homogeneous sphere shaped ZnDTO particles

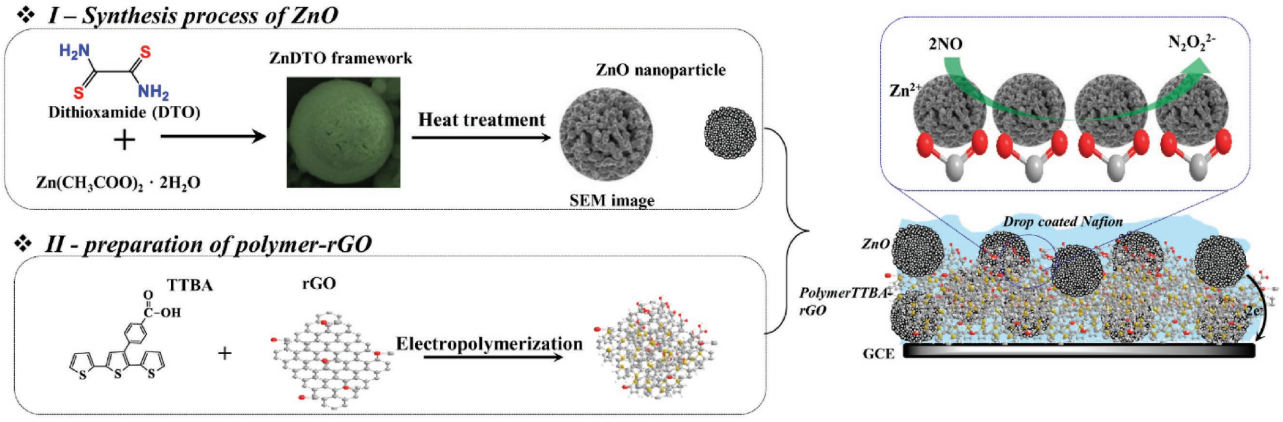

Figure 1. Schematic nitric oxide sensor based on the polymer-rGO/ZnO electrode.

in two different particle sizes (**Figure 2**a,c). The smaller particles were obtained by controlling the reaction time and their size in the range of 900 ± 50 nm, whereas the larger particles were obtained at longer reaction time and their size was calculated to be 3000 ± 100 nm. After pyrolysis of ZnDTO, TEM image of smaller ZnO NPs revealed a porous sphere structured particle (Figure 2b); similarly, the FESEM images of the larger size particles revealed the sphere shape of the ZnO NPs (Figure 2d). It should be noted that the size of the both smaller and bigger ZnO NPs almost remained its parent one after pyrolysis. The porosity in the ZnO NPs is due to the evaporation of organic elements (C, N, and S) from ZnDTO through the oxidation process in the presence of air during pyrolysis. Finally, the remaining Zn converts to porous ZnO NPs. Porosity of the ZnO material was confirmed by the Barrett-Joyner-Halenda (BJH) pore size distribution method (Figure S1, Supporting Information). This indicated that ZnO NPs had bimodal pore size distribution such as mesoporous (3–15 nm) and macroporous (50–200 nm). These mesoporous and macroporous were appeared in homogeneous spherical structure of ZnO NPs, which helped to access electrolyte inside the NPs and resulted in the reduction of NO effectively.[26] The atomic percentage of ZnO was confirmed by EDX measurements and it reveals 50.27% of Zn and 49.73% of O; the ratio of both elements is almost 1:1 (Figure 2e). In step II, the TTBA-rGO complex was electropolymerized on the glassy carbon (GC) electrode by three times potential cycling between 0.0 and 1.4 V. Finally, the ZnO NPs were drop coated on the poly(TTBA-rGO) electrode to obtain a final surface of poly(TTBA-rGO)/ZnO. Even other Zn based MOFs, such as zeolitic imidazolate framework (ZIF-8), MOF-5, and bimetallic ZIFs,[27] can be used to prepare ZnO, these compounds, however, may have different morphology, various metal contents, and different surface porosity than that of ZnDTO-derived ZnO. Thus, they may show somewhat different or comparable catalytic activity to the present study.

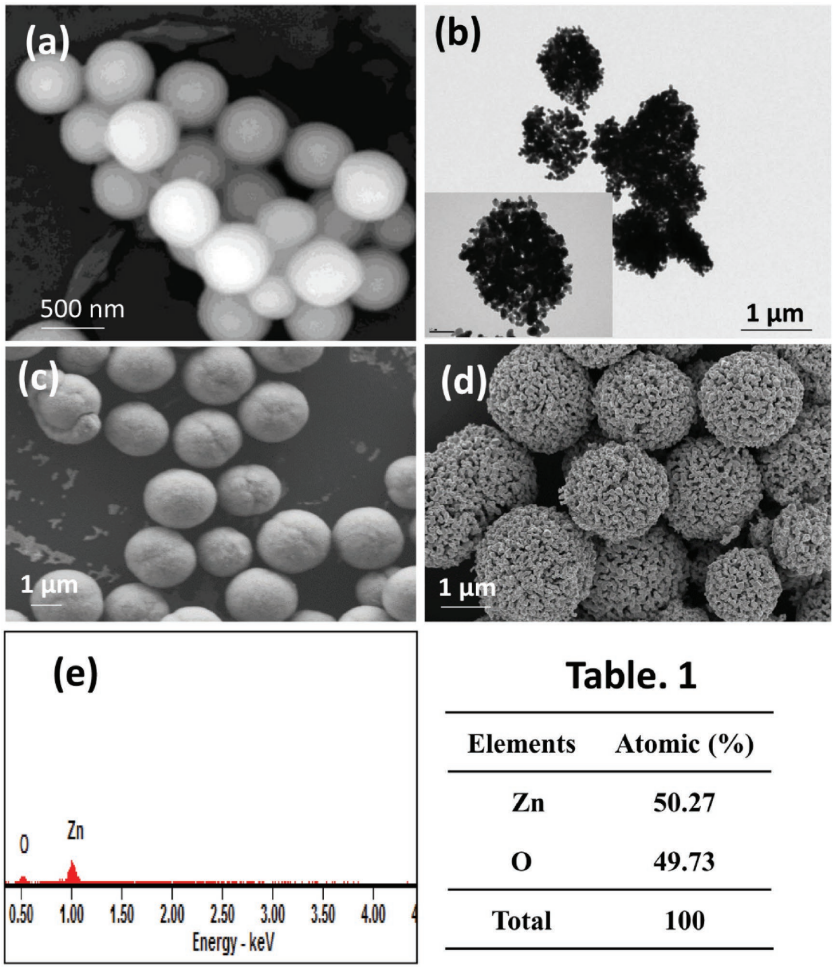

Table. 1

Elements	Atomic (%)
Zn	50.27
O	49.73
Total	100

Figure 2. FESEM images for a,b) small and c,d) bigger sized ZnDTO and ZnO. (e) EDX and elements analysis for ZnO.

2.2. Characterization of the Poly(TTBA-rGO)/ZnO

The XRD analysis was carried out and it provided the information of crystallinity and phase components of the modified electrodes (Figure S2a, Supporting Information). The diffraction peaks of prepared ZnO are in good agreement with the standard XRD spectrum of ZnO (JCPDS No. 89-1397). No diffraction peaks for impurity were observed, indicating the ZnDTO was completely transformed to ZnO. For poly(TTBA-rGO), a broad diffraction peak of reduced graphene oxide (rGO) was observed at the 2θ value of 26.2°. A similar peak was also observed along with ZnO diffraction peaks in poly(TTBA-rGO)/ZnO sample, and the peaks of ZnO at poly(TTBA-rGO)/ZnO sample were slightly broader compared to only ZnO peaks, which indicates the interference between the poly(TTBA-rGO) and ZnO.

Furthermore, XPS measurements were performed to investigate the electronic structure and the chemical interaction of ZnO and poly(TTBA-rGO). As shown in Figure S2b (Supporting Information), the survey spectrum displayed that the characteristic peaks of all the elements (Zn, C, S, and O) for ZnO NPs, poly(TTBA-rGO), and poly(TTBA-rGO)/ZnO samples confirm the formation of a composite layer on the electrode surface. The deconvoluted XPS spectrum for ZnO with two peaks located at 1045.2 eV for Zn 2p1/2 and 1022.1 eV for Zn 2p3/2 (**Figure 3**a) reveals the characteristic of Zn^{2+}. However, there was a small shift in the binding energy (0.3 eV) of Zn for the poly(TTBA-rGO)/ZnO layer. The O 1s peaks corresponding to the oxygen groups in the ZnO NPs appeared at binding energies of 532.4 and 530.3 eV (Figure 3b). For poly(TTBA-rGO) layer, the oxygen peaks from the 3′-(p-benzoic acid)-2,2′:5′,2″-terthiophene (TTBA) polymer exhibited at 533.2 and 532.5 eV. However, there was small shifting in the oxygen peak positions (0.4 eV) for the poly(TTBA-rGO)/ZnO layer compared to ZnO oxygen peaks, due to the interaction of oxygen groups of ZnO NPs with polymer nanocomposite. Figure 3c shows the deconvoluted spectra of S 2p for the poly(TTBA-rGO)/ZnO sample, further confirming the polymer layer on the electrode surface. Deconvoluted XPS spectra of C 1s for poly(TTBA-rGO) showed peaks at 284.6 eV for C−C, 285.07 eV for C−OH, and 289.0 eV for C−C=O, whereas the same peaks were also observed for poly(TTBA-rGO)/ZnO layer at binding energies of 284.1 eV for C−C, 285.24 eV for C−OH, and 288.45 eV for C−C=O (Figure 3d). Shifting in the binding energy on the poly(TTBA-rGO)/ZnO layer toward lower values suggests the interaction and synergetic effect between the ZnO NPs with rGO-supported terthiophene polymer composite. In addition, the binding energy shifts of both Zn and C−OH group of polyTTBA to the high energy indicate that there is an interaction between the Zn^{2+} ion and the carboxylic acid group of polyTTBA during the formation of the composite.

The morphologies of modified electrodes were characterized by FESEM. **Figure 4**a displays the FESEM image of poly(TTBA)-modified electrode, showing the surface structure of polymer network with small particles. Figure 4b reveals the structure of only rGO layers. It can be seen from Figure 4c that a combined structure of poly(TTBA) network and rGO sheets on the electrode surface confirms the formation of poly(TTBA-rGO) nanocomposite layer. The FESEM image of the final layer that was ZnO NPs immobilized on poly(TTBA-rGO) suggested that ZnO NPs have completely covered the electrode surface (Figure 4d). EDX

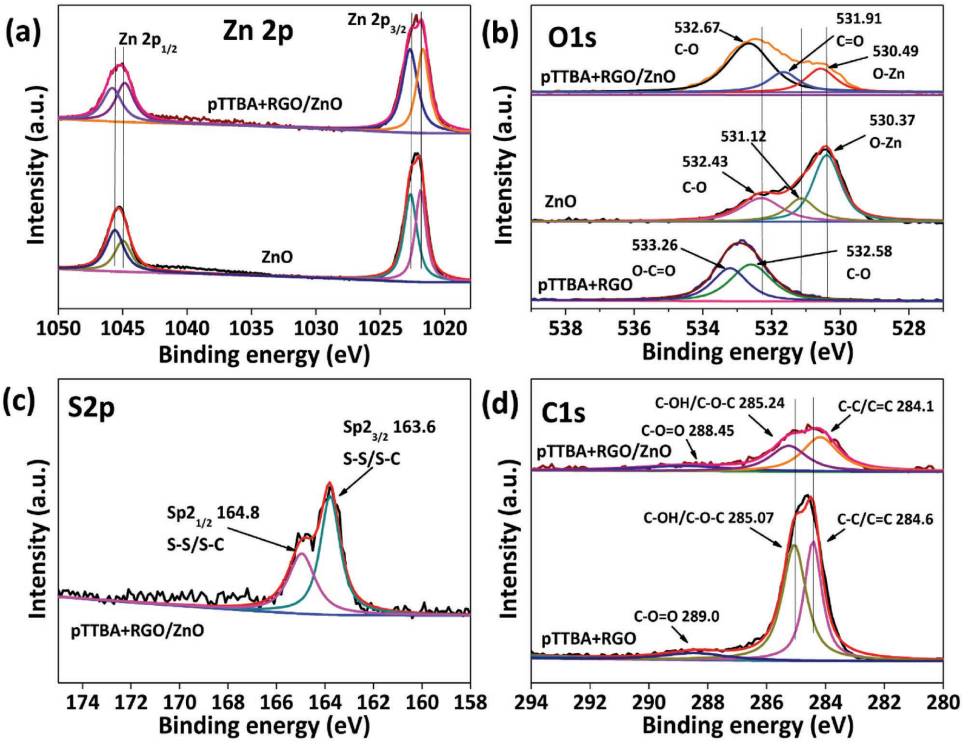

Figure 3. Deconvoluated XPS spectra for ZnO, poly(TTBA-rGO), and poly(TTBA-rGO)/ZnO; a) Zn 2p, b) O1s, c) S2p, and d) C1s.

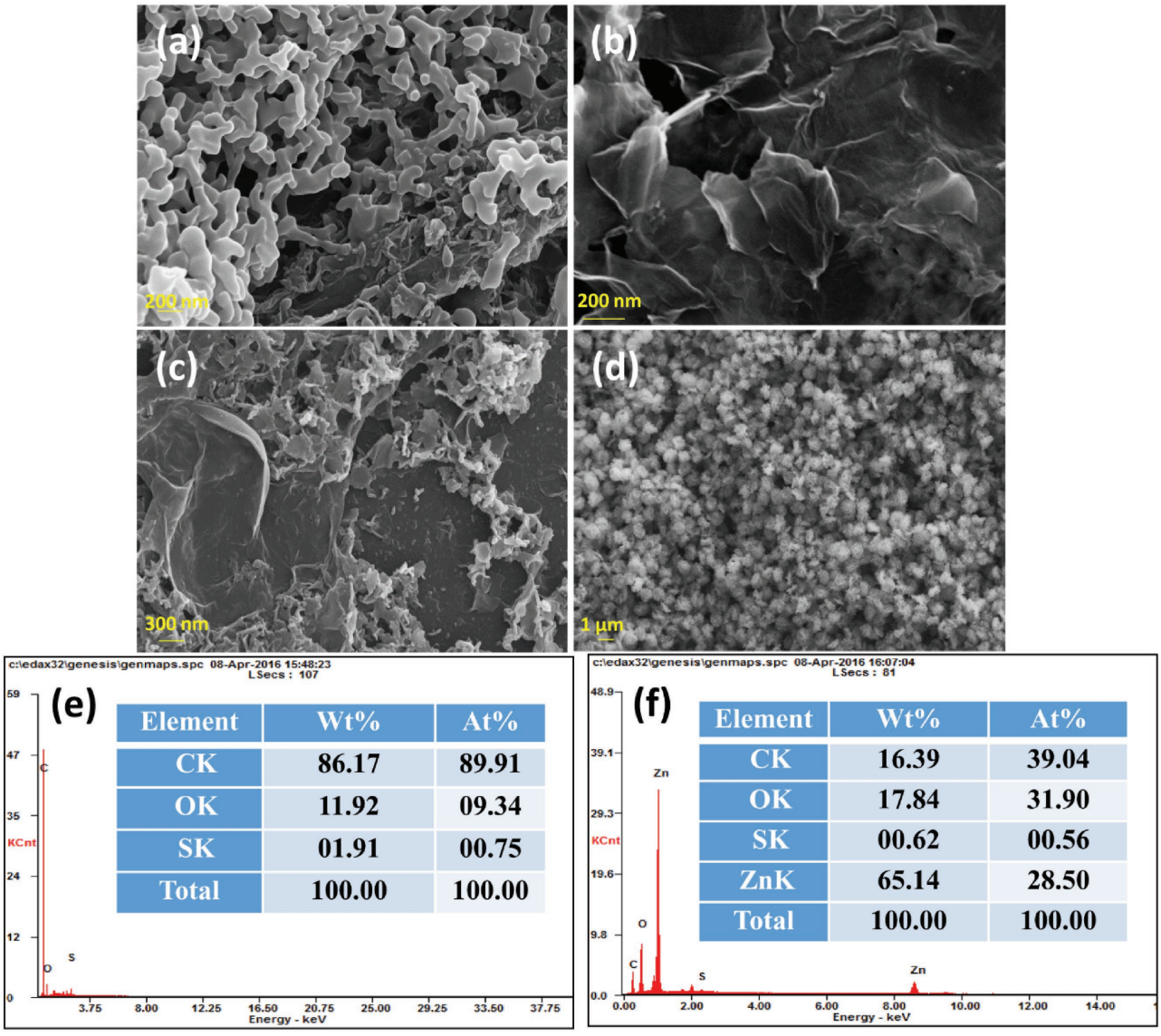

Figure 4. FESEM images for a) poly(TTBA), b) rGO, c) poly(TTBA-rGO), and d) poly(TTBA-rGO)/ZnO. EDX and elemental analysis for e) poly(TTBA-rGO) and f) poly(TTBA-rGO)/ZnO.

results demonstrate the presence of C, O, and S elements in poly(TTBA-rGO) and C, O, S, and Zn in poly(TTBA-rGO)/ZnO electrodes, and it confirmed the presence of elements on both the electrodes. Further, the modification of the electrode was confirmed by EDX mapping images (Figure S3, Supporting Information). It suggested the uniform distribution of C, S, O, and Zn from polymer and rGO composites on the electrode surface; single ZnO NP was selected for the mapping analysis to easily understand the elements distribution in ZnO NP.

2.3. Voltammetric and Impedance Characterization of the Modified Electrodes

CV study using potassium ferricyanide is a convenient tool for surface characterization of the modified electrodes, where the charge transfer at the interface between electrolyte and electrode must occur either by a barrier or through defects. CVs of bare GC, polyTTBA, poly(TTBA-rGO), ZnO, and poly(TTBA-rGO)/ZnO modified electrodes in 4.0×10^{-3} M $Fe[(CN)_6]^{3-/4-}$ solution containing 0.1 M KCl as a supporting electrolyte at the scan rate of 50 mV s^{-1} is presented in **Figure 5**a. Well-defined oxidation and reduction peaks for the Fe^{3+}/Fe^{2+} redox couple at the bare glassy carbon electrode (GCE) were observed. The ZnO-modified GCE exhibited increased peak currents compared to the bare GCE; this might be due to the much surface area of ZnO as that enhances the peak currents. The poly(TTBA)-modified electrode demonstrated less current as compared to all the modified layers. This is mainly because of the negative charge repulsion between the carboxylic groups and negatively charged ferricyanide ions. However, with the addition of rGO, i.e., poly(TTBA-rGO) electrode increased the peak currents as compared to poly(TTBA) layer, suggesting the increased charge transfer process due to the presence

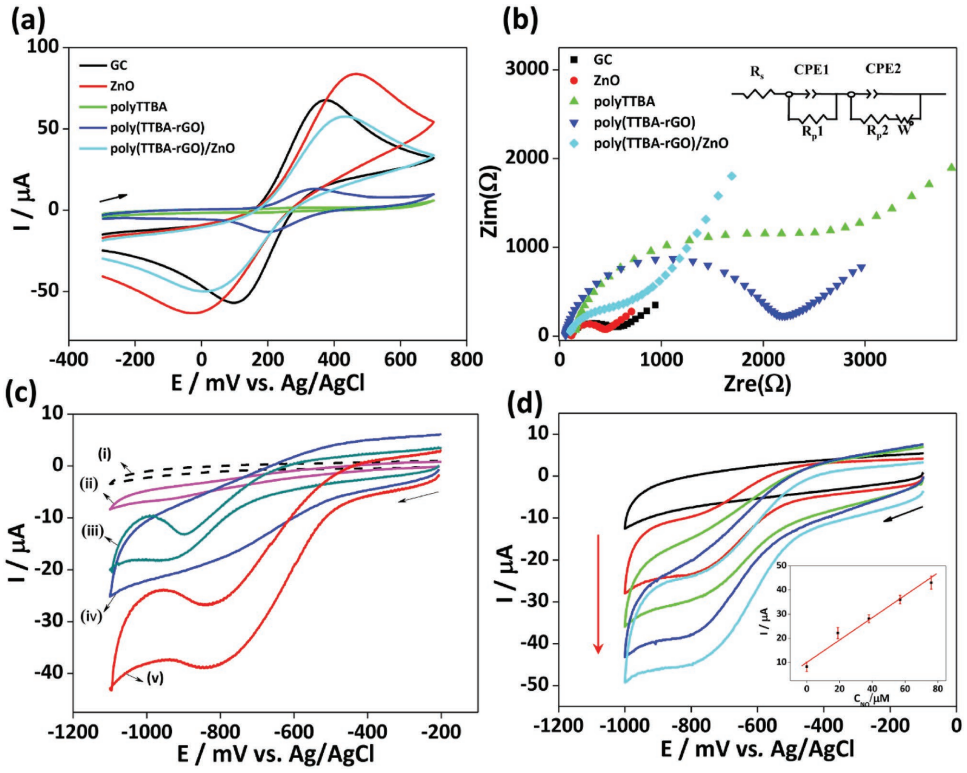

Figure 5. a) CVs and b) EIS in 4×10^{-3} M of $[Fe(CN)_6]^{4-/3-}$ for GC, ZnO, poly(TTBA), poly(TTBA-rGO), and poly(TTBA-rGO)/ZnO. c) CVs for (i) GC (ii) poly TTBA (iii) ZnO (iv) poly (TTBA+rGO) nanocompposite and (v) poly(TTBA+rGO)/ZnO-modified GC electrodes 57.0×10^{-6} M of NO in 0.1 M PBS (pH7.0) at a scan rate of 50 mV s^{-1}. Inset: Concentration. d) CVs of poly(TTBA-rGO)/ZnO for different concentration of NO.

of highly conductive rGO. Furthermore, the increased peak currents at poly(TTBA-rGO)/ZnO electrode illustrate that the modified electrode possesses better electrocatalytic activity than poly(TTBA) and poly(TTBA-rGO) electrodes. The lesser current for poly(TTBA-rGO)/ZnO as compared to the ZnO-modified electrode is due to the presence of poly(TTBA). The presence of a polymer gives the advantage to maintain the stable surface where the metal oxide NPs are normally not stable on a bare GC substrate.

EIS was employed for further determining the interfacial charge transfer properties of modified electrodes, where it was measured for all the modified electrodes presenting in Figure 5b. The semicircular portion at the higher frequencies region represents the charge transfer-limited process and the semicircle diameter corresponds to the charge transfer resistance (R_{ct}). The bare GCE exhibits a smaller semicircle with the R_{ct} value of 520 Ω, implying the characteristic of a diffusional controlled step of the electrochemical process. The ZnO-modified electrode displayed the R_{ct} values of 410 Ω, suggesting a good charge transfer process. The poly(TTBA) and poly(TTBA-rGO)-modified electrodes display semicircles with R_{ct} values of 2650 and 1930 Ω, respectively, which indicates the presence of polymer that makes interfacial charge transfer more difficult and it decreased by the addition of rGO. However, poly(TTBA-rGO)/ZnO electrode exhibits a smaller semicircle with R_{ct} value of 960 Ω, which is smaller than poly(TTBA) and poly(TTBA-rGO) electrodes; this may be ascribed to the combining properties of ZnO and polymer-rGO composite layer.

2.4. Detection of NO

To minimize the interference effect on the poly(TTBA-rGO)/ZnO electrode for the detection of NO, 0.1% Nafion was coated to the sensor surface,[28] where the concentration of Nafion did not affect the sensitivity of the sensor probe. All subsequent experiments were performed with the Nafion-coated sensor probe. The NO reduction ability of the modified electrodes was first examined by CV in 0.1 M phosphate buffered saline (PBS) containing 57.0×10^{-6} M of NO at the potential range of –0.2 to –1.1 V with a scan rate of 50 mV s^{-1}. The CVs recorded for bare GC, poly(TTBA), ZnO, poly(TTBA-rGO), and poly(TTBA-rGO)/ZnO electrodes are shown in Figure 5c. As can be seen, no peaks are observed for the bare GC, poly(TTBA), and poly(TTBA-rGO)-modified electrodes, suggesting that these electrodes do not have any catalytic property toward the reduction of NO. However, the ZnO-modified electrode exhibits a cathodic peak at –0.90 V corresponding to the reduction of NO, which confirms the electrocatalytic activity of ZnO toward the reduction of NO. Interestingly, the poly(TTBA-rGO)/ZnO electrode demonstrates the positive shifting of peak potential (–0.81 V) and the enhanced current response for NO reduction as compared to the pristine ZnO electrode. Such a highest activity arises from the combined property of stable polymer layer, high conductivity of rGO, and electrochemical activity of ZnO made of poly(TTBA-rGO)/ZnO as an excellent probe for NO detection. In addition, CVs at different concentrations of NO on the poly (TTBA-rGO)/ZnO electrode were

measured (Figure 5d), which implied that the reduction current density increased with the increased concentration of NO. The sensor performance of poly(TTBA-rGO)/ZnO electrode was evaluated using different loading of ZnO NPs (Figure S4, Supporting Information). It demonstrated that 0.01 mg of ZnO was the best composition to get the highest current response of NO reduction. The same composition was used for the subsequent experiment. To demonstrate the influence of particle size for NO reduction, the sensor probe was modified with two different sizes of ZnO NPs, and CVs were performed in PBS solution containing 19.0×10^{-6} M NO (Figure S5, Supporting Information). The smaller sized ZnO (900 ± 50 nm)-modified electrode exhibited larger reduction current and the most positive potential for NO reduction. The electrode modified with larger ZnO (3000 ± 100 nm) demonstrated lesser current response and the peak potential of NO reduction was more negative. It reveals that smaller sized ZnO has better catalytic activity; therefore, subsequent experiments were carried out using the small size ZnO NPs (poly(TTBA-rGO)/ZnO)-modified electrode. CVs were recorded for the reduction of NO using poly(TTBA-rGO)/ZnO electrode at the scan rates between 5 and 200 mV s^{-1} (Figure S6, Supporting Information). The reduction peak current of NO increased linearly with the root mean square of scan rates with a correlation coefficient of 0.997. This indicates that the process of electrode reaction is diffusion controlled.

2.5. Optimization of Analytical Parameters for NO Detection

The analytical parameters were examined for the detection of NO using poly(TTBA-rGO)/ZnO probe in terms of applied potential, pH, and temperature. The applied potential was optimized from the potential range between –0.6 and –1.0 V; it exhibited the maximum current at –0.95 V (Figure S7a, Supporting Information). Therefore, –0.95 V was selected as a suitable applied potential for the amperometric measurements of NO. The effect of pH was investigated in the range between 2.0 and 9.0. As shown in Figure S7b (Supporting Information), the current response was increased in the acidic condition for NO reduction; however, it was slightly decreased at neutral pH (7.0) and became constant over pH 8.0. For the practical analysis of biological samples, pH 7.0 was used as an optimum condition. The temperature effect was also studied from 10 to 50 °C. The current response was increasing constantly with temperature up to 35 °C; later for increased temperature, the current response became constant (Figure S7c, Supporting Information). For the practical purpose and for real-time measurements, all the experiments were performed at room temperature.

2.6. Amperometric Response of the Poly(TTBA-rGO)/ZnO Sensor Probe

The amperometric *i–t* curve was recorded for the detection of NO at the poly(TTBA-rGO)/ZnO-modified electrode at an applied potential of –0.95 V upon successive addition of NO to the N_2 gas saturated 0.1 M PBS (pH = 7.0). The typical amperometric response for the sensor probe is presented in **Figure 6**a. It shows that small sized ZnO modified (poly(TTBA+rGO)/ZnO-900 nm) electrode proves to have an enhanced amperometric response for NO detection as compared with bigger sized ZnO modified (poly(TTBA+rGO)/ZnO-3 µm) electrode. It was observed that the sensor probe quickly responded to the change of NO concentration and achieved a steady-state current level. Figure 6b exhibits the corresponding calibration plot for both the electrodes, indicating that it shows great sensitivity at poly(TTBA+rGO)/ZnO (900 nm) electrode. There are two segments in the relevant linear range for the detection of NO at both the electrodes, which are 19 to 171×10^{-9} M and 228×10^{-9} M to 76×10^{-6} M for poly(TTBA+rGO)/ZnO (900 nm) electrode and 38 to 171×10^{-9} M and 228×10^{-9} M to 76×10^{-6} M for poly(TTBA+rGO)/ZnO (3 µm). The linear regression equation for poly(TTBA+rGO)/ZnO (900 nm) is $i_p(\mu A) = (-1.56 \pm 0.06) + (0.98 \pm 0.006)$ [C] ($\times 10^{-6}$ M) with correlation coefficient of 0.996 and $i_p(\mu A) = (-0.72 \pm 0.016) + (1.924 \pm 0.039)$ [C] ($\times 10^{-6}$ M) with correlation coefficient of 0.947. The linear regression equation for poly(TTBA+rGO)/ZnO (3 µm) was of $i_p(\mu A) = (-1.10 \pm 0.02) + (0.96 \pm 0.002)$ [C] ($\times 10^{-6}$ M) with correlation coefficient of 0.959 and $i_p(\mu A) = (-0.52 \pm 0.013) + (1.38 \pm 0.03)$ [C] ($\times 10^{-6}$ M) with correlation

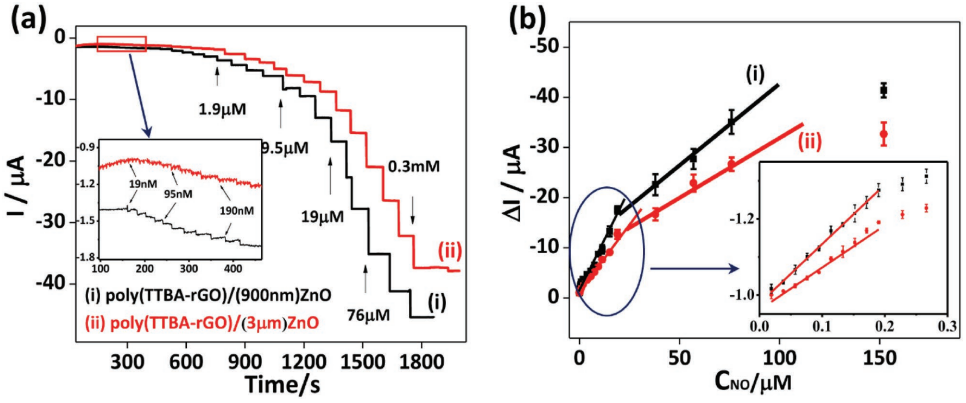

Figure 6. a) Amperometric responses and b) corresponding calibration graphs of 900 nm and 3 µm sized ZnO modified poly(TTBA+rGO)/ZnO electrodes to successive addition of NO into N_2 saturated PBS solution.

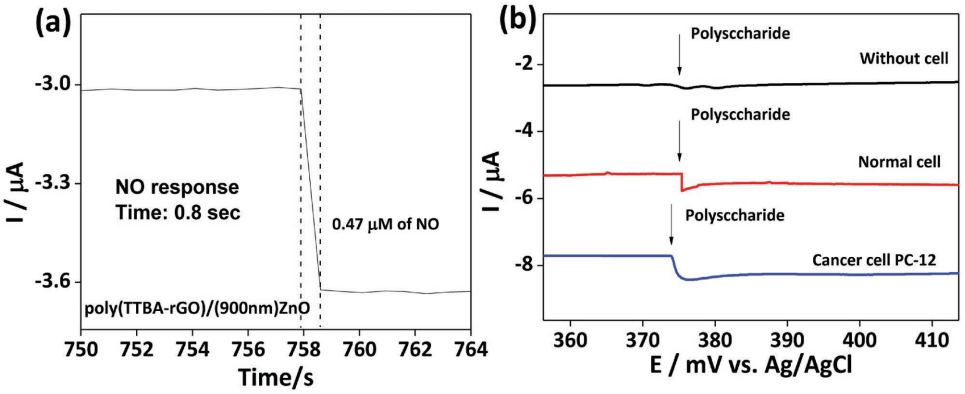

Figure 7. a) Amperometric response time of the sensor probe at an NO concentration of 0.47×10^{-6} M. b) Amperometric response of the poly(TTBA-rGO)/ZnO electrode for (i) without cells, (ii) normal cells, and (iii) with PC-12 cancer cells with the addition of 50×10^{-6} M polysaccharide.

coefficient of 0.992. The detection limit was calculated to be $7.7 \pm 0.43 \times 10^{-9}$ M for poly(TTBA+rGO)/ZnO (900 nm) and $25 \pm 5 \times 10^{-9}$ M for poly(TTBA+rGO)/ZnO (3 µm) electrodes ($n = 3$, $k = 3$). The results indicate an excellent performance for the small size ZnO NP modified electrode and it reveals that the small particle size results in achieving low detection limit, wide linear range, and high sensitivity for NO detection. The amperometric response time of the poly(TTBA-rGO)/ZnO electrode for NO detection was within 0.8 s (**Figure 7**a). The proposed sensor is comparable with other enzymatic and nonenzymatic sensors (Table S1, Supporting Information), and it was also very adequate at monitoring NO levels in the living cell lines. The long-term durability test was performed using five different sensors for 50 d (Figure S8, Supporting Information). The sensitivity of the sensors retained more than 96.0% of their initial response for 40 d when stored at room temperature.

2.7. Interference Studies

To prove the selectivity, the anti-interference ability of the sensor probe is an important analytical factor. The Nafion-coated poly(TTBA-rGO)/ZnO electrode helps to remove the interference from the oxygen species and biological interference species.[26] The sensor probe displayed only negligible amount of current difference (only 6.5%) as compared to the without Nafion-coated electrode (Figure S9, Supporting Information). The selectivity of the poly(TTBA-rGO)/ZnO sensor probe with Nafion coating was evaluated in the presence of common biological interference species in their physiological concentration level. Figure S10 (Supporting Information) displays the chronoamperometric response at the potential of –0.95 V for the species including 1.0×10^{-3} M ascorbic acid, 1.0×10^{-3} M acetaminophen (AP), 10×10^{-6} M superoxide (O_2^-), 10×10^{-6} M hydrogen peroxide (H_2O_2), 1.0×10^{-3} M L-arginine, and 1×10^{-3} M uric acid along with the addition of 1.9×10^{-6} M of NO; there was no interference from these species for NO detection. This indicated high selectivity of the Nafion-coated poly(TTBA-rGO)/ZnO electrode, which completely eliminated the interferences during NO detection. This result demonstrates that the selectivity of the proposed sensor probe toward NO detection is excellent.

2.8. Measurements of NO Release from Living Cells

Cancer and normal cells were cultured in a T75 cell culture flask up to a final concentration of 7.5×10^6 cells mL^{-1} to detect NO released from them. The excess NO release from the cells was triggered by the addition of polysaccharide. It is well known that the macrophage cells stimulated by polysaccharide can generate NO with an expression of inducible NO synthase.[29] The half-life of NO released from living cells is very short (<10 s), so a quick measurement of NO is important in biological systems.[30] Chronoamperometry was used to monitor the current response generated by the NO reduction, which was released from the cells, at an applied potential of –0.95 V. Curves (i) (cancer cells) and (ii) (normal cells) in Figure 7b depict the amperometric response of poly(TTBA-rGO)/ZnO electrode in the presence of cells. After the addition of polysaccharide to the cells in PBS solution, it was allowed to stand for 10 min to permit the maximum release of NO. The change in current response indicates the NO release from the cells (Figure 7b). To validate the current response for NO released from the cells, a control experiment was performed by adding polysaccharide to only PBS ((iii) without cells); no change in the current was observed, indicating the absence of electrochemical signal for polysaccharide. This study suggests that the poly(TTBA-rGO)/ZnO electrode can be a promising sensor probe for NO detection in real-time operations of physiological and pathological investigations.

3. Conclusion

We have developed a high-performance electrochemical NO biosensor based on porous ZnO NPs, which has been derived from a ZnDTO framework, and polyterthiophene-rGO composite. The porous structure of the ZnO was characterized by FESEM and TEM measurements, and two different sized particles were prepared. By taking advantage of the synergetic effect between ZnO and poly(TTBA-rGO) nanocomposite layer, the sensor probe displayed excellent electrocatalytic activity and explored to detect NO released from normal and cancer cell lines. Due to the instability of ZnO layer, we synthesized the TTBA-rGO composite on

the electrode surface and then ZnO was immobilized, which resulted in the stable surface and excellent performance that can detect NO in nanomolar level. The sensing performance of the both different-sized ZnO NPs was measured and the results revealed the excellent performance for the smaller sized ZnO modified electrode. This suggested the importance of the particle size to achieve the excellent electrocatalytic activity. For in vitro detection of NO in living cells, the proposed sensor probe was subjected to distinguish a trace amount of NO from normal and cancer cells. It was observed that cancer cells showed the highest response current as compared to normal cells. Thus, this study holds great potential for the diagnosis of cancer diseases.

4. Experimental Section

Materials: Graphite powder was purchased from Sigma-Aldrich (USA) and used without further purification. Tetrabutylammonium perchlorate (TBAP, electrochemical grade) was obtained from the FlukaCo. (USA) and dried under vacuum (10^{-5} Torr). All aqueous solutions were prepared in double-distilled water, which was obtained from a Milli-Q water purifying system (18 MΩ cm). Disodium hydrogen phosphate, sodium dihydrogen phosphate, AP, AA, dopamine, sodium chloride, $[Fe(CN)_6]^{3-}$, $[Fe(CN)_6]^{4-}$, Nafion (5 wt% solution in a mixture of lower aliphatic alcohols and water), dimethylformamide (DMF), and acetonitrile (≥99.8%, anhydrous, sealed under N_2 gas) were supplied from Sigma-Aldrich Co. A PBS solution was prepared by modifying 0.1 M of disodium hydrogen phosphate with the mixture of 0.1 M of sodium dihydrogen phosphate with 0.1% sodium chloride. All other chemicals were of extra pure analytical grade and used without further purification.

Instruments: The morphology of the prepared material and electrode surface was confirmed by FESEM (Zeiss SUPRA25), and the atomic ratio of the electrode and elemental mapping was measured by EDX. XRD (Thermo Fisher Scientific, UK) and XPS (Multilab 2000 instrument, Thermo Fisher Scientific, UK) were used to examine the chemical nature and interaction of the prepared materials and modified electrodes at the Korea Basic Science Institute (Busan).The CV and chronoamperometry were obtained using a Kosentech bipotentiostat (Model Bipot-1, South Korea) in a three-electrode system with modified GC (area 0.07 cm^2) as the working electrode, platinum wire as the auxiliary electrode, and silver/silver chloride (Ag/AgCl, saturated KCl) as the reference electrode. An EG&G Princeton Applied Research PARSTAT 2263 instrument was used to measure the EIS at open circuit voltages from 100.0 to 0.1 kHz (AC amplitude 10.0 mV). Before electrochemical experiments, GC electrode was polished using three different alumina slurries and washed with distilled water and then dried.

Preparation of Electrode Materials: As a precursor for ZnO NPs, ZnDTO was prepared using two separate DMF solvents containing 0.250 g (0.00207 mol) of DTO and 0.456 g (0.00207 mol) of Zn acetate with 0.5 g of polyvinylpyrrolidone (PVP). Both solutions were mixed with stirring at 80 °C. The reaction mixture was kept for incubation at the same temperature. Small sized particles were collected by terminating the reaction for 1 h. For bigger sized particles, the incubation time was continued up to 8 h. Final compounds were obtained by centrifugation and washed with ethanol several times and vacuum dried at 50 °C. For the preparation of ZnO NPs, the prepared different particle sized ZnDTO was transferred to a quartz boat and placed in a tube furnace. The temperature of the furnace was heated up to 700 °C at the heating rate of 3 °C min^{-1} and the same temperature was maintained for 3 h under open air condition. The GO was prepared by a modified Hummer's method.[31] The freshly prepared GO was dispersed in water and it was reduced by adding hydrazine hydrate at 100 °C with stirring and it was continued for 24 h to obtain rGO. The TTBA monomer was prepared by a previously reported method.[32]

Preparation of Sensor Probe: The sensor probe was fabricated by electropolymerization of TTBA-rGO complex followed by drop coating of ZnO NPs. For instance, acetonitrile containing TTBA monomer and rGO were well sonicated to obtain a clear dispersion of TTBA-rGO complex. The obtained TTBA-rGO complex was mixed with 0.1 M TBAP and it was subjected for electropolymerization on the GC electrode by cycling the potential between 0.0 and 1.4 V for three times at a scan rate of 100 mV s^{-1} to form a poly(TTBA-rGO) composite electrode. After polymerization, the poly(TTBA-rGO) electrode was washed with acetonitrile to remove freely bonded monomer and rGO. For the poly(TTBA-rGO)/ZnO electrode, 1 mg of ZnO NPs was dispersed in 1 mL of water and 5 µL of the dispersion was pipetted out on poly(TTBA-rGO) electrode and dried at 30 °C for 12 h, followed by drop coating of 0.1 % Nafion solution. For comparison, only polymer film electrode was prepared using only monomer solution. For ZnO NP electrode, it was prepared by drop coating of ZnO NP dispersion on GC electrode.

Cell Culture and Detection of NO Released from Living Cells: The cancerous PC-12 and the normal HEK-293 were cultured in a high glucose Dulbecco's modified eagles medium supplemented with 1% penicillin-streptomycin and 10% fetal bovine serum. The cultures were maintained in an incubator at 37 °C with 5% CO_2 under 95% humidity. The media in the cultures was replaced regularly to avoid the changes in the pH and to provide ample supplements for the growing cells until a 95% confluency was obtained. The cells were then removed from the culture by trypsinization and washed with dulbecco's PBS to remove any remaining serum or trypsin. The resulting cells were then suspended in a known volume of Dulbecco's phosphate buffered saline (DPBS) to get a proper number of cells per milliliter. To detect the NO released from the cells, they were stimulated with an external precursor, lipopolysaccharide, which initiates the release of excess NO from them. The amount of NO released from cancer and normal cells was sensitively detected using the proposed poly(TTBA-rGO)/ZnO sensor surface.

Supporting Information

Supporting Information is available from the Wiley Online Library or from the author.

Acknowledgements

M.-Y.K. and M.H.N. contributed equally to this work. This work was supported by the National Research Foundation of Korea (NRF) grant funded by the Korea government (MSIP) (Grant No. 2015R1A2A1A13027762).

Conflict of Interest

The authors declare no conflict of interest.

[1] V. Bauer, R. Sotnikova, *Gen. Physiol. Biophys.* **2010**, *29*, 319.
[2] D. S. Bredt, S. H. Snyder, *Neuron* **1992**, *8*, 3.
[3] F. L. Ricciardolo, P. J. Sterk, B. Gaston, G. Folkerts, *Physiol. Rev.* **2004**, *84*, 731.
[4] M. Kelm, *Biochim. Biophys. Acta* **1999**, *1411*, 273.
[5] F. Bedioui, D. Quinton, S. Griveau, T. Nyokong, *Phys. Chem. Chem. Phys.* **2010**, *12*, 9976.
[6] C. Csonka, T. Páli, P. Bencsik, A. Görbe, P. Ferdinandy, T Csont, *Br. J. Pharmacol.* **2015**, *172*, 1620.
[7] R. Trouillon, *Biol. Chem.* **2013**, *394*, 17.
[8] W. C. A. Koh, M. A. Rahman, E. S. Choe, D. K. Lee, Y. B. Shim, *Biosens. Bioelectron.* **2008**, *23*, 1374.
[9] J. O'M. Bockris, S. U. M. Khan, *Surface Electrochemistry*, Plenum Press, New York **1993**.
[10] X. W. Sun, Y. Yang, *ZnO Nanostructures and their Applications*, Taylor & Francis Group LLC, Boca Raton **2012**.
[11] a) J. F. Zhang, C. M. Li, X. Q. Cui, J. X. Wang, X. W. Sun, H. Dong, C. Q. Sun, *Electroanalysis* **2007**, *19*, 1008; b) P. Zhu, Z. Y. Weng, X. Li, X. M. Liu, S. L. Wu, K. W. K. Yeung, X. B. Wang, Z. D. Cui, X. J. Yang, P. K. Chu, *Adv. Mater. Interfaces* **2016**, *3*, 1500494.
[12] G. W. She, X. Huang, L. L. Jin, X. P. Qi, L. X. Mu, W. S. Shi, *Small* **2014**, *10*, 4685.
[13] B. Gu, C. Xu, C. Yang, S. Liu, M. Wang, *Biosens. Bioelectron.* **2011**, *26*, 2720.
[14] A. Kołodziejczak-Radzimska, T. Jesionowski, *Materials* **2014**, *7*, 2833.
[15] R. R. Salunkhe, J. Tang, Y. Kamachi, T. Nakato, J. H. Kim, Y. Yamauchi, *ACS Nano* **2015**, *9*, 6288.
[16] H. Furukawa, K. E. Cordova, M. O. Keeffe, *Science* **2013**, *341*, 1230444.
[17] S. M. Park, in *Handbook of Organic Conductive Molecules and Polymers*, Vol. *3* (Ed: H. S. Nalwa), Wiley, Chichester **1997**.
[18] M. A. Rahman, P. Kumar, D. S. Park, Y. B. Shim, *Sensors* **2008**, *8*, 118.
[19] D. M. Kim, H. B. Noh, Y. B. Shim, *J. Electrochem. Sci. Technol.* **2013**, *4*, 125.
[20] D. M. Kim, H. B. Noh, D. S. Park, S. H. Ryu, J. S. Koo, Y. B. Shim, *Biosens. Bioelectron.* **2009**, *25*, 456.
[21] *New Progress on Graphene Research* (Ed: L. R. Gong), InTech Publishing Co, Rijeka, Crotia **2013**.
[22] A. Ambrosi, C. K. Chua, A. Bonanni, M. Pumera, *Chem. Rev.* **2014**, *114*, 7150.
[23] K. Zhao, X. Q. Yan, Y. S. Gu, Z. Kang, Z. M. Bai, S. Y. Cao, Y. C. Liu, X. H. Zhang, Y. Zhang, *Small* **2016**, *12*, 245.
[24] Y. L. Chen, Z. A. Hu, Y. Q. Chang, H. W. Wang, Z. Y. Zhang, Y. Y. Yang, H. Y. Wu, *J. Phys. Chem. C* **2011**, *115*, 2563.
[25] a) M. H. Naveen, K. B. Shim, Md. S. A. Hossain, J. H. Kim, Y. B. Shim, *Adv. Energy Mater.* **2016**, *7*,1602002; b) K. Kanaizuka, R. Haruki, O. Sakata, M. Yoshimoto, Y. Akita, H. Kitagawa, *J. Am. Chem. Soc.* **2008**, *130*, 15778.
[26] P. Wu, J. Wang, C. He, X. Zhang, Y. Wang, T. Liu, C. Duan, *Adv. Funct. Mater.* **2012**, *22*, 1698.
[27] Y.-Z. Chen, C. Wang, Z.-Y. Wu, Y. Xiong, Q. Xu, S.-H. Yu, H.-L. Jiang, *Adv. Mater.* **2015**, *27*, 5010.
[28] W. C. A. Koh, M. A. Rahman, E. S. Choe, D. K. Lee, Y.-B. Shim, *Biosens. Bioelectron.* **2008**, *23*, 1374.
[29] S. Chen, D. K. Yin, W. B. Yao, Y. D. Wang, Y. R. Zhang, X. D. Gao, *Acta Pharmacol. Sin.* **2009**, *30*, 1008.
[30] Y. L. Liu, X. Y. Wang, J. Q. Xu, C. Xiao, Y. H. Liu, X. W Zhang, J. T. Liu, W. H. Huang, *Chem. Sci.* **2015**, *6*, 1853.
[31] D. C. Marcano, D. V. Kosynkin, J. M. Berlin, A. Sinitskii, Z. Sun, A. Slesarev, L. B. Alemany, W. Lu, J. M. Tour, *ACS Nano* **2010**, *4*, 4806.
[32] P. Chandra, H.-B. Noh, M.-S. Won, Y. B. Shim, *Biosens. Bioelectron.* **2011**, *26*, 4442.

Received: February 14, 2017
Revised: March 21, 2017
Published online: